Fabrication and analysis of phantoms providing the equal-image-density for basic experiment of next-generation-type X-ray diagnosis

Poster No.: C-0012
Congress: ECR 2016
Type: Scientific Exhibit
Authors: N. Kimoto[1], H. Hayashi[1], H. Okino[1], K. Takegami[1], I. Maehata[1], Y. Kanazawa[1], T. Yamakawa[2], S. Yamamoto[3]; [1]Tokushima/JP, [2]Osaka/JP, [3]Kanagawa/JP
Keywords: Image verification, Technical aspects, Dosimetry, Diagnostic procedure, Experimental, Conventional radiography, Radioprotection / Radiation dose, Radiation physics
DOI: 10.1594/ecr2016/C-0012

Aims and objectives

X-ray equipment is widely used for diagnosis in the medical field. It requires short examination time, and this characteristic leads to many examinations with only a small burden to patients. Using traditional radiography systems, signal (contrast) of the image is determined by the products of the energy and quantity of X-rays. Therefore, when the products of linear attenuation coefficient and thickness are similar among the materials the same digital value is obtained. The situation is schematically explained in **Fig. 1**, and in reality the contamination rate from scattered X-rays plays an important role. Identification of the materials is valuable for X-ray diagnosis, therefore it becomes problem that the same digital values are obtained when different materials are measured with the traditional system. Recently a photon counting system is attracting attention in the medical field **[1-4]**, because the system has energy resolving capability. The X-ray spectrum shown in **Fig. 1** shows the schematic drawing of the typical photon counting system which can measure three energy regions. Using them, it is expected that information about the attenuation coefficients can be derived, namely the materials will be identified by analyzing the spectrum. At present, the system has been progressing, but currently a fundamental study is needed. In the diagnostic X-ray examination, the digital value is affected by, kind of materials, the contamination rate from the scattered X-ray and the heel effect. When we fabricate the "equal-image-density materials" which give the same digital values, evaluation of the sensitivity analysis for the contamination rate from scattered X-ray **[5]** and heel effect **[6]** is needed.

Figure 2 shows the aim of this study; to fabricate equal-image-density materials necessary for basic experiment of a photon counting system and to analyze the materials in term of the influence on the contamination rate from scattered X-ray and heel effect on the obtained image. These data are valuable in the study of a photon counting system.

The chart of our study is presented in **Fig. 3**. There are two different process; one is fabrication of equal-image-density materials, and the other is experimental procedure for measuring the contamination rate from the scattered X-ray and the heel effect. Each process of our study is represented in the chart.

Images for this section:

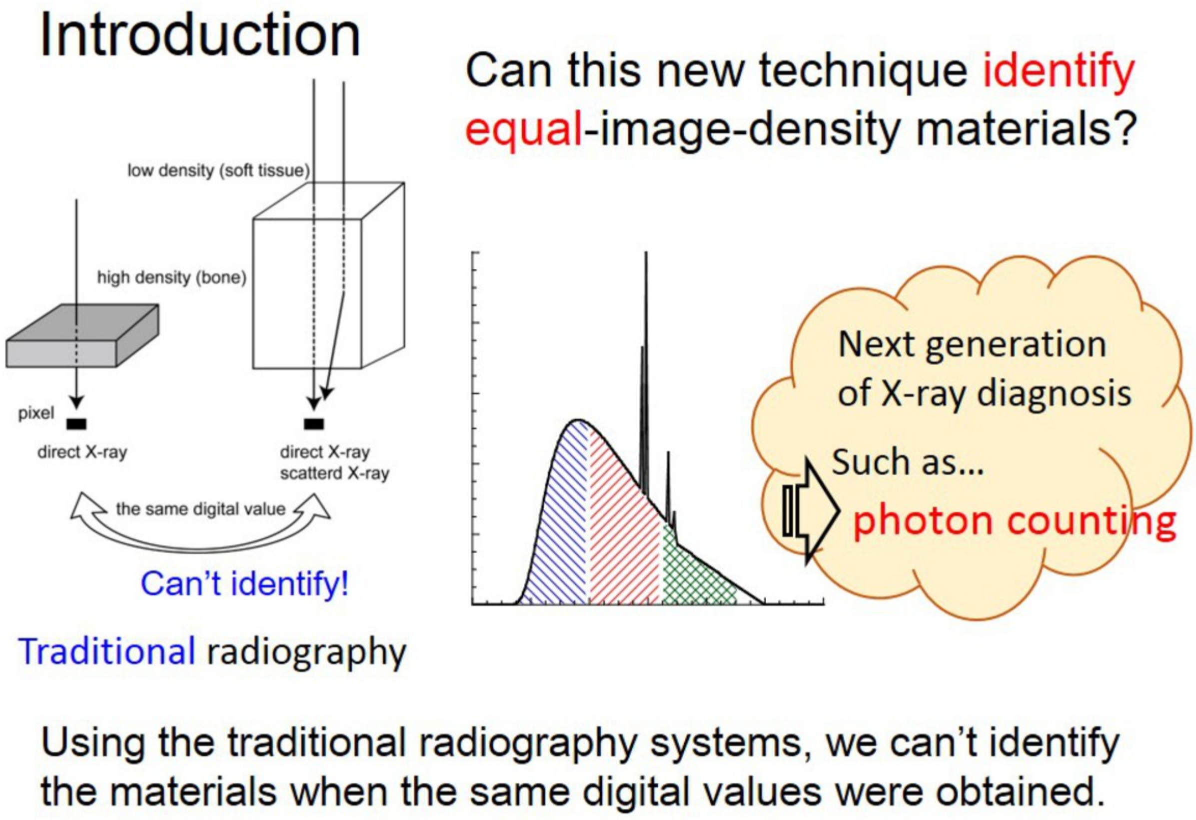

Fig. 1: Introduction of our study. Using a traditional system, on occasion when different materials are measured, the same digital value can be obtained.

© - Tokushima/JP

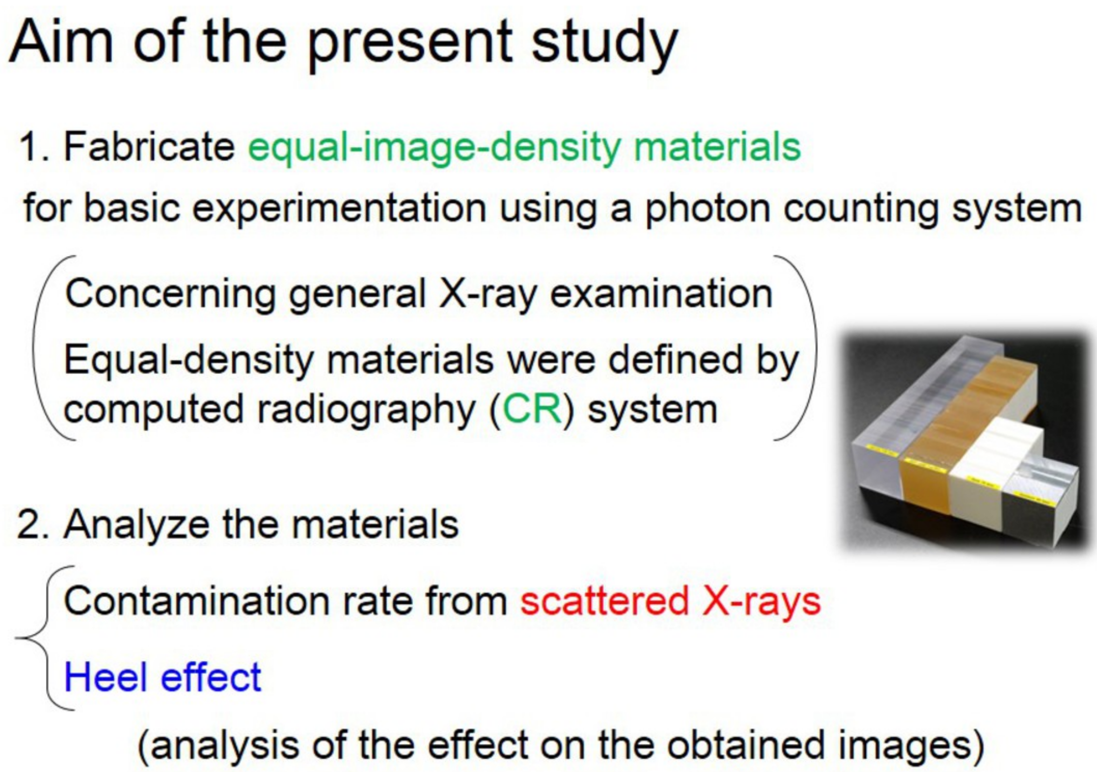

Fig. 2: The aim of the present study: to fabricate equal-image-density materials, and to analyze them in terms of contamination rate from scattered X-ray and heel effect on the obtained image.

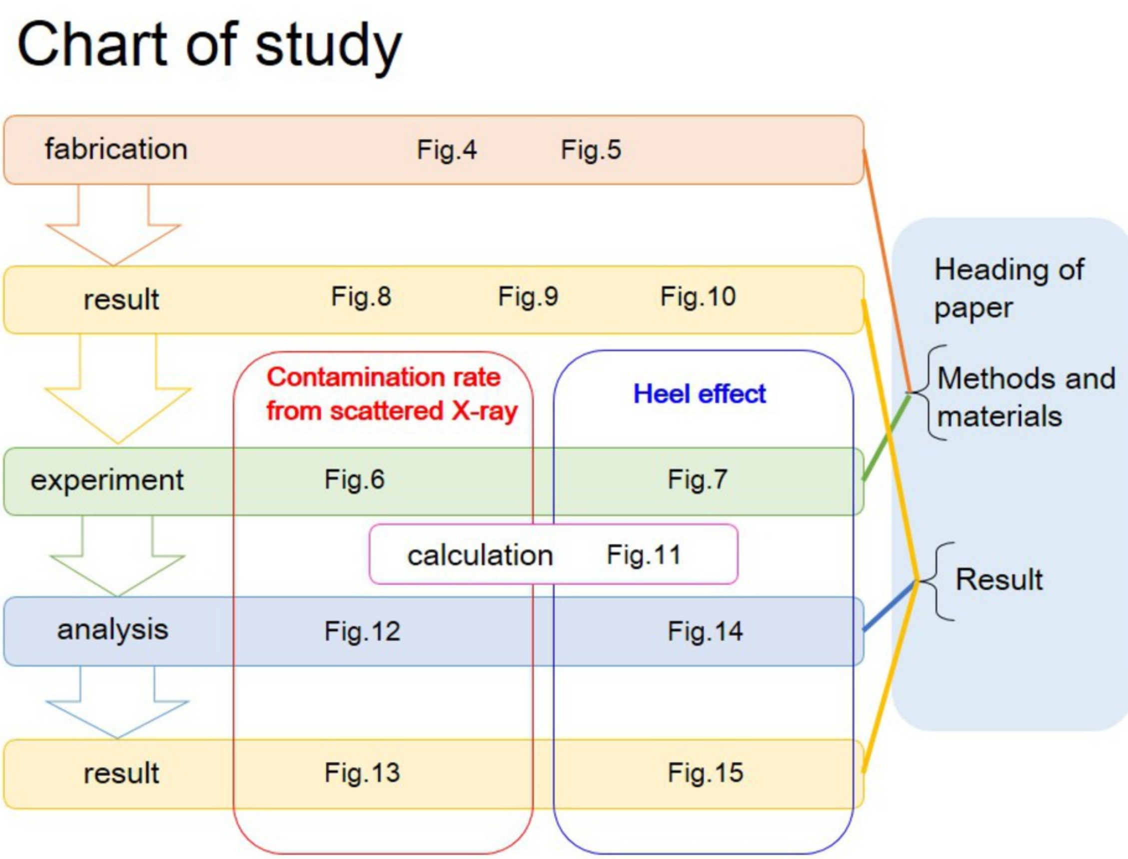

Fig. 3: Chart of our study. The process of fabricating equal-image-density materials and the details of the materials are presented in figures 4-5, 8-10. Furthermore we investigate the influence of contamination rate from scattered X-ray and heel effect using our fabricated materials, as shown in figures 6-7, 11-15.

© - Tokushima/JP

Methods and materials

Figure 4 shows the procedure for fabricating the equal-image-density materials. First, we prepared soft tissues-equivalent material (SZ-207, Kyoto Kagaku Ltd., Kyoto, Japan) having thicknesses of 20 mm, 40 mm, 80 mm and 160 mm. They are used as a standard; namely, the thickness of other materials will be determined so as to obtain the same digital value with those of the standard materials. Second, we prepared aluminum, acrylic and bone-equivalent material (BE-H, Kyoto Kagaku Ltd., Kyoto, Japan) having certain thicknesses. Then, the thickness of these materials were modified in accordance to the following procedure; first, we took the X-ray image, second, we measured digital values of it, and third, we plotted the digital value as a function of phantom thickness. These processes were iterated until the digital value became the same as that of the standard. As described above, aluminum, acrylic and bone-equivalent material, giving the same digital value with soft tissues-equivalent material, were fabricated.

Figure 5 shows process of fabricating the equal-image-density materials using machine tools. We prepared rods having cross-sectional surfaces of 40 mm square. The materials (rods) were cut piece by piece using a circular saw and then finely ground down using a boring machine.

Figure 6 shows the schematic drawing for measuring of the contamination rate from scattered X-rays. We applied the collimator method proposed by Hayashi *et al*. **[5]**. The experimental setup consists of diagnostic X-ray equipment (Toshiba Medical Systems Corporation, MRAD-A 50S/70), CR (computed radiography) system (phosphor plate: RP-4S, Konica Minolta Health Care Co., Ltd., Tokyo, Japan), and collimators having diameters 5-30 mm. The collimators were composed of a lead plate being 2 mm in thickness supported by aluminum. Distance between phosphor plate and collimator, X-ray equipment are 20 cm and 100 cm, respectively. Tube voltages are 40kV and 100 kV and tube current-time products are 10 mAs in 40kV, and 0.5 mAs in 100 kV.

Figure 7 shows a schematic drawing of measurement of the heel effect **[6]**. The heel effect appeared in differences of X-ray spectra of which X-rays emitted for orientation of the long axis of the X-ray tube; the maximum difference was presented between the directions of anode and cathode. When we used an 8 inch phosphor plate under typical clinical conditions (source to image receptor distance of 100 cm), the solid angle became 5 degrees. Hence, we examined the influence of X-ray image caused by the heel effect using the following three settings; as shown in **Fig. 7**, "Normal position" uses X-rays on the center, "Cathode side" uses X-rays differed from central axis by 5 degrees, and "Anode side" uses X-rays in the opposite direction of "Cathode side".

Images for this section:

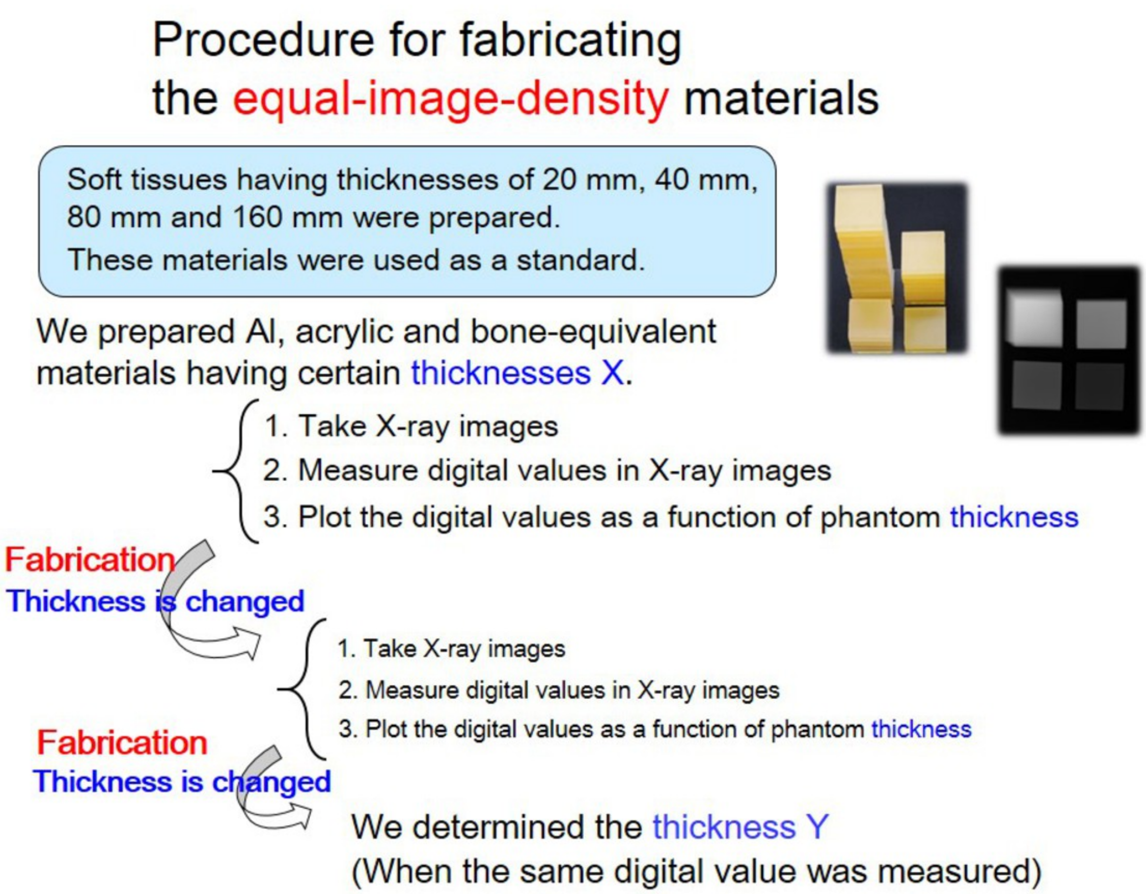

Fig. 4: Procedure for fabricating the equal-image-density materials. We prepared commercially available materials of soft tissue, bone, acrylic and aluminum. The thickness which gives the same digital value in X-ray image was determined by the procedure described in the figure.

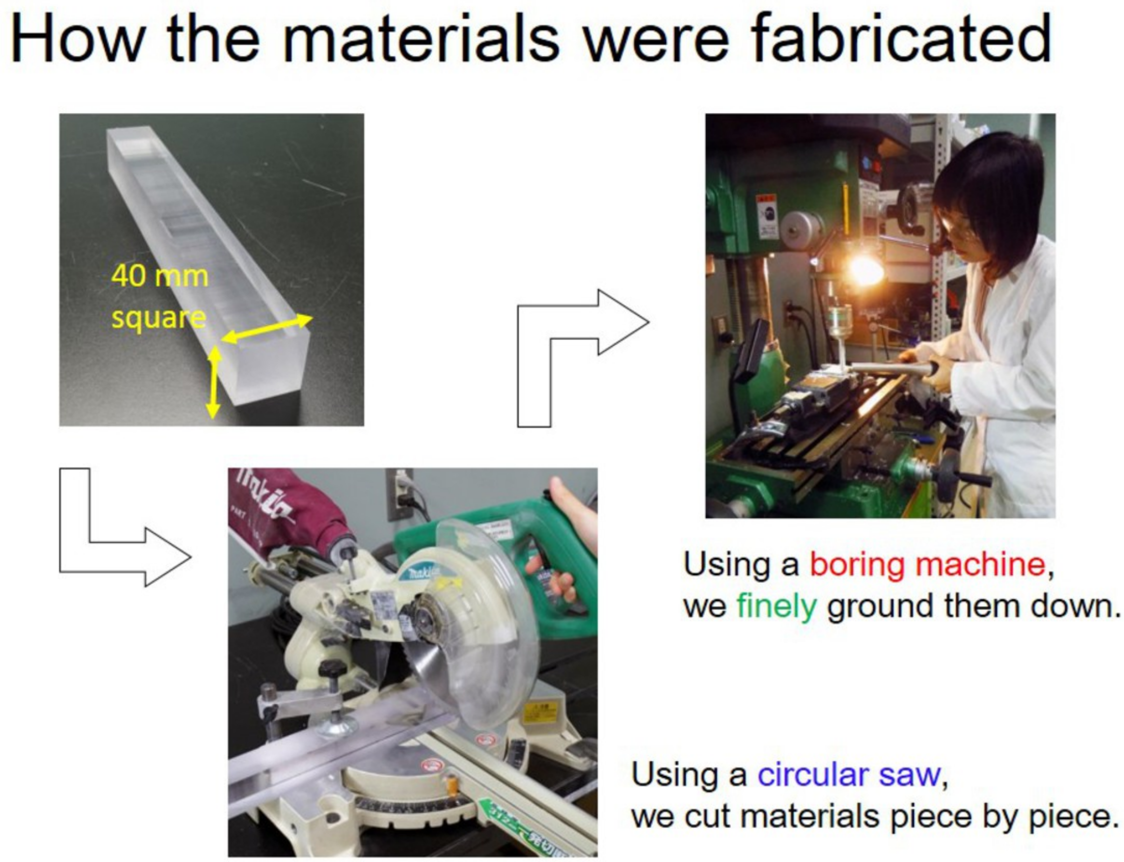

Fig. 5: The procedure used to fabricate materials by means of machine tools. At first, samples were cut roughly using a circular saw, and then ground down finely using a boring machine.

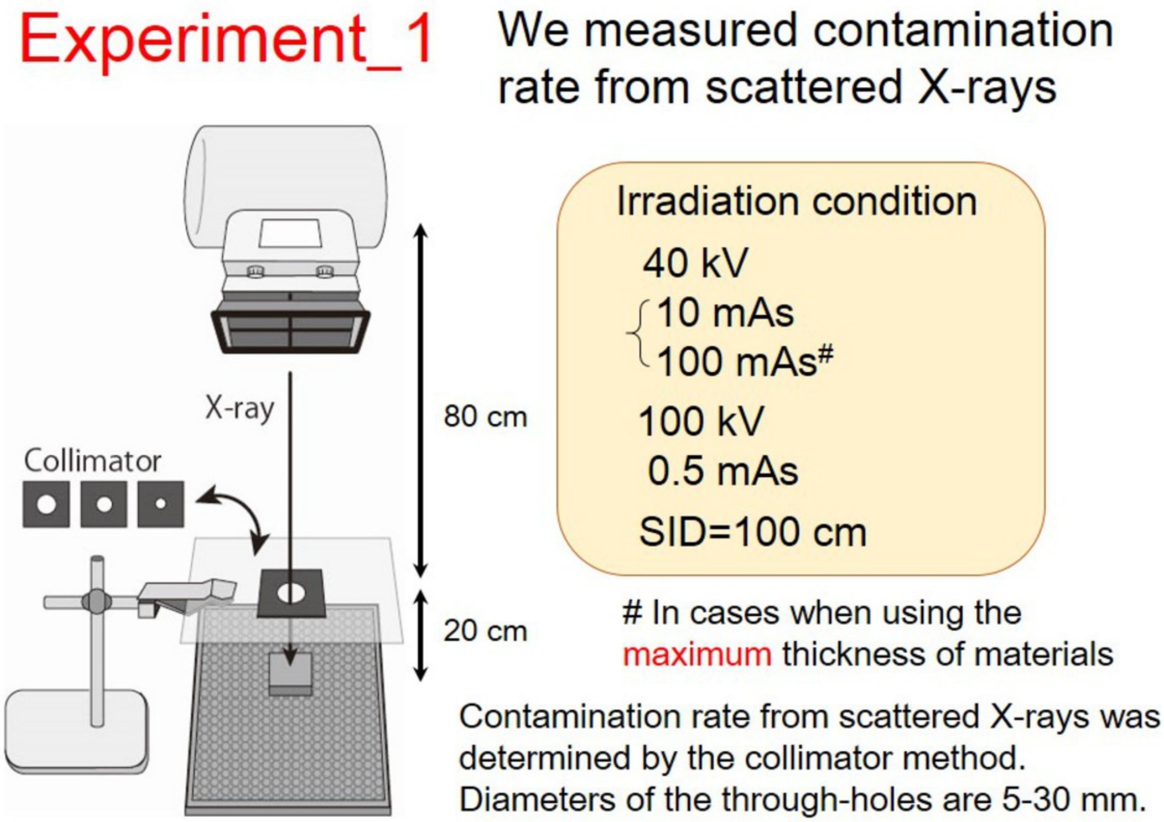

Fig. 6: Schematic drawing of experiment to measure contamination rate from scattered X-ray. The irradiation condition is indicated in the figure.

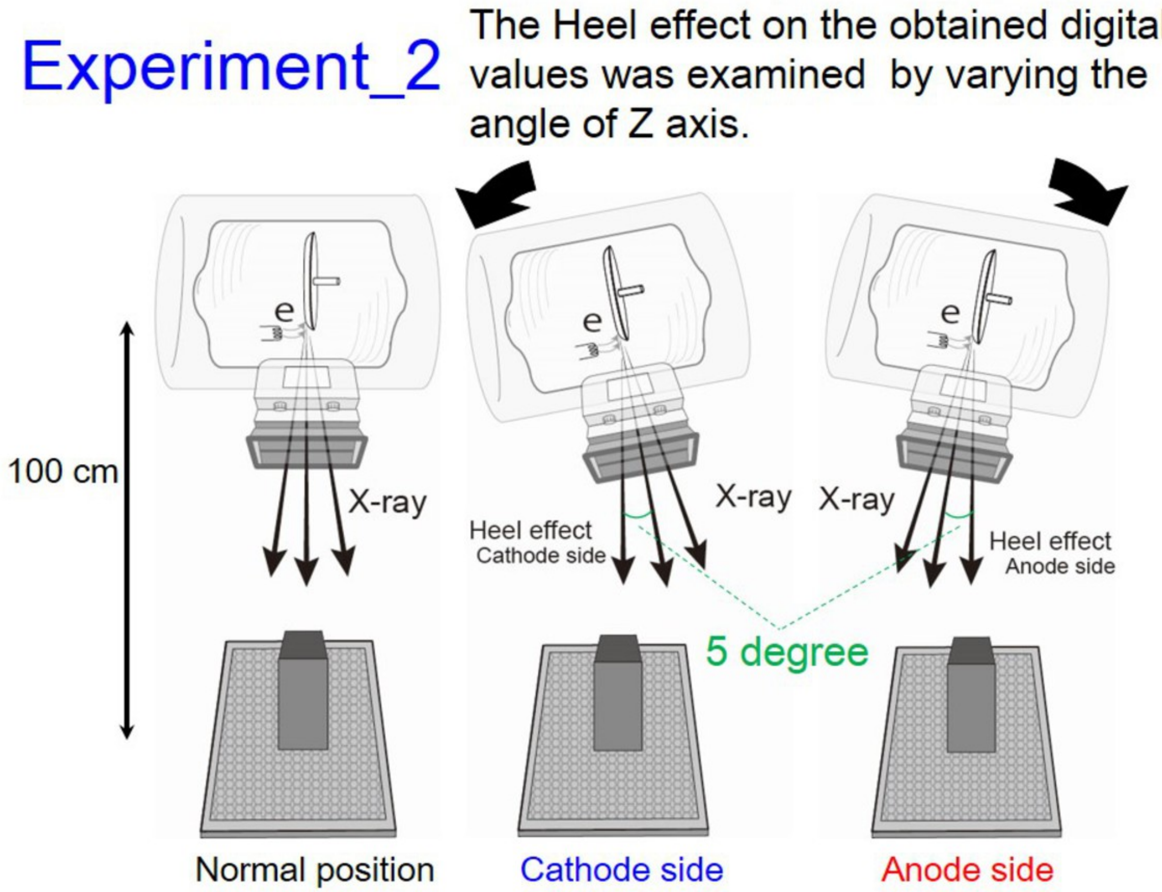

Fig. 7: Schematic drawings of experiments to evaluate heel effect on the obtained image. By tilting X-ray equipment at an angle of 5 degrees, corresponding X-ray images were obtained in cathode and anode sides.

Results

Figure 8 shows a typical example of fabricated materials. The graph represents relationship between thickness of materials and digital value measured with CR system. There are linear relationships between thickness and digital value as indicated by the solid line. In this case, the standard material having thickness of 80 mm represents a digital value of 1660, and we found that bone being 35.3 mm thick gives the same digital value. Results for all fabricated samples were summarized in **Fig. 9**. Left and right figures show results of 40 kV and 100 kV X-rays, respectively. Trends for soft tissue and acrylic are most of the same, and those of aluminum and bone are similar.

Figure 10 shows a summary of fabricated materials. Left figure shows photograph; the materials on the left side are soft tissue adopted as standard, the materials made of acrylic, bone and aluminum in the middle show equal-image-density materials at 40 kV X-ray, and the right is at 100 kV X-ray. The right table shows detailed information of thickness. The materials in the same row belong to a group of equal-image-density material. The upper half rows indicate equal-image-density material for 40 kV X-ray and the lower are for 100 kV.

The calculation methodology for intensity from digital value using a CR system is shown in **Figure 11**. The obtained X-ray image was analyzed by ImageJ software **[7]** and the measured digital value was converted into intensity using the input-output characteristic of the CR system **[8,9]**. In the analysis of contamination rates from scattered X-ray and the heel effect, the calculated intensity described above was also used.

In order to explain the analysis procedure, we exemplify the analysis of contamination rate from scattered X-ray of soft tissue. The contamination rate from scattered X-ray was measured by collimator method as represented in the right figure of **Fig. 12**; first, experimental values (intensities) concerning different diameters were measured, second, they were normalized by the data without collimator (whole of the upper surface of the phantom was irradiated) and plotted as a function of collimator size, third, extrapolated value (fraction of direct X-ray) concerning collimator size of 0 mm was derived, finally, the contamination rate from scattered X-ray was determined by subtracting "the fraction of direct X-ray" from 1. The left figure of **Fig. 12** summarizes the contamination rate from scattered X-ray for thicknesses of 20 mm, 40 mm, 80 mm and 160 mm.

In a similar way, the collimator method was applied to all fabricated materials. The results were summarized in **Fig. 13**. The upper and lower columns show condition of 40 kV X-rays and 100 kV X-rays, respectively. As the thicknesses of materials increased, the more contamination rate from scattered X-ray increased. The numerical values were 8-60 % for 40 kV X-rays and 10-53 % for 100 kV X-rays.

We exemplify the analysis methodology of heel effect using **Fig. 14**. On the left, schematic drawings of the experimental setup and corresponding X-ray image are presented. In the normal position, all of the phosphor plate was irradiated. On the other hand, only a part of the phosphor plate was irradiated in the cathode and anode positions. Measured intensities for the three different positions were normalized by that corresponding to the normal position. In the right figure of **Fig. 14**, the dependences of the intensities are plotted as a function of phantom thickness; blue and red symbols indicate the results of the cathode and anode sides, respectively. In the present case for 40 kV X-rays, the maximum differences from the normal position are found to be 5% and 13% for the cathode and anode sides, respectively.

In a similar way, the analyses were applied to the all materials and they were summarized in **Fig. 15**. The figures in the upper and lower columns show conditions of 40 kV X-rays and 100 kV X-rays, respectively. The heel effect affected on the intensity difference was 1-15 % for 40 kV X-rays and 0.1-9 % for 100 kV X-rays.

Images for this section:

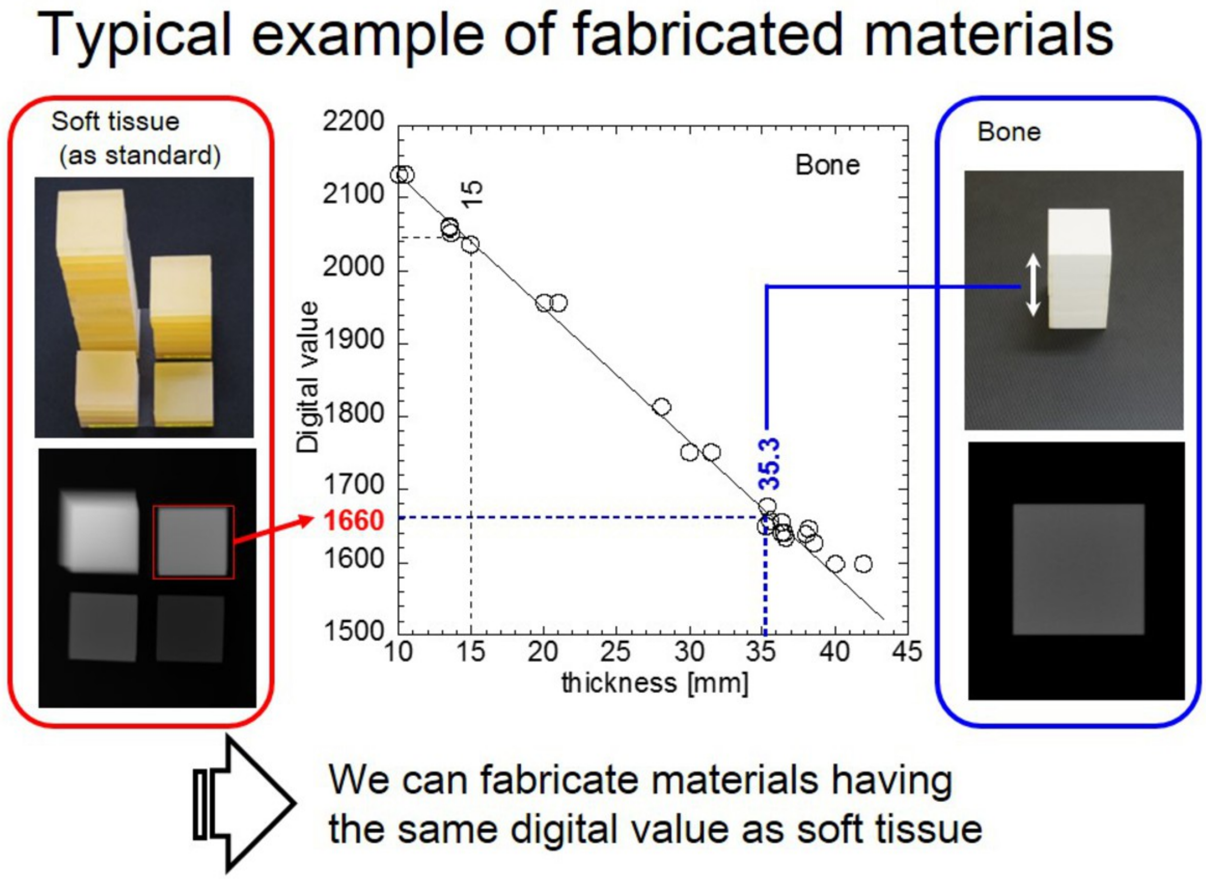

Fig. 8: Typical example to determine the thickness of fabricated materials. The proper thickness of fabricated materials which gives the same digital value with that of the standard material was determined.

Relationship between material thickness and digital value

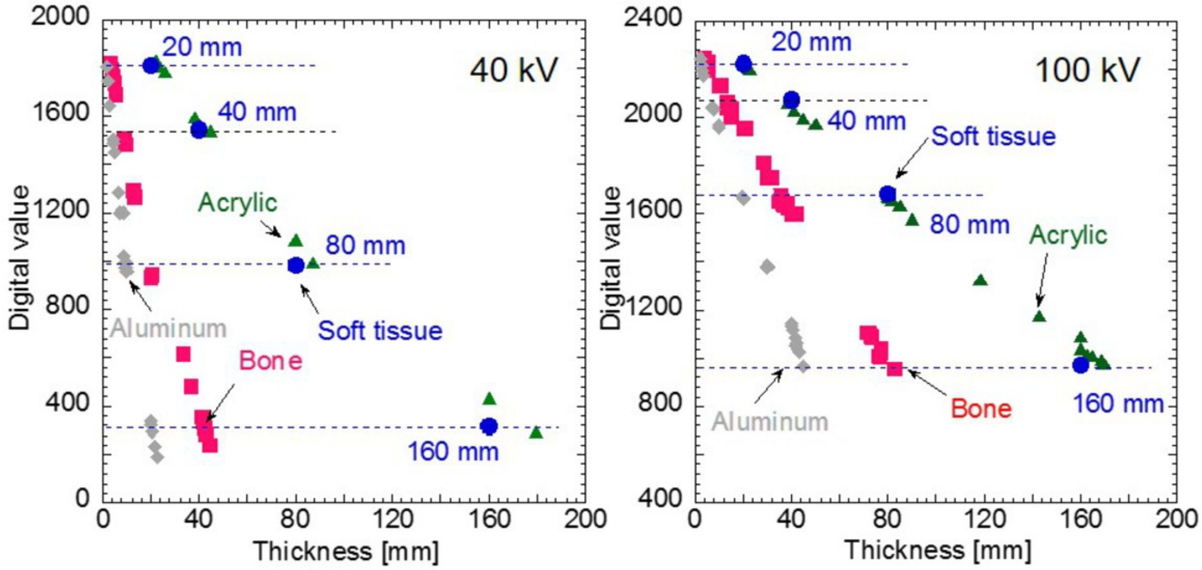

Fig. 9: Relationship between material thickness and digital value for all fabricated materials. Trends for soft tissue and acrylic are most of the same, and those of aluminum and bone are similar.

Summary of the fabricated equal-image-density materials

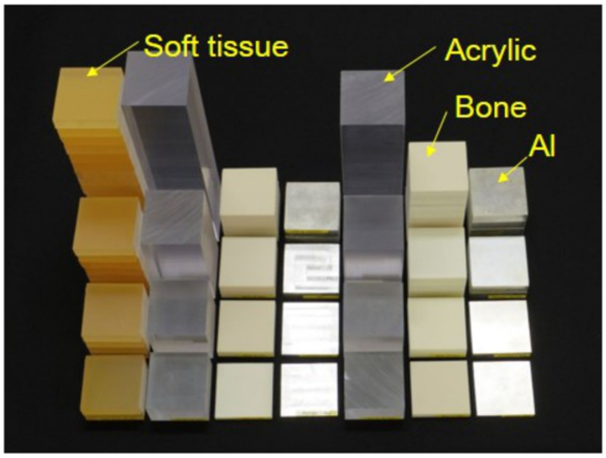

Photo: fabricated materials

Tube voltage	Thickness[mm]			
	Soft Tissue	Acrylic#2	Al#2	Bone#2
40 kV	20	24	1.9	4.1
	40	44.4	4.1	9.1
	80	87.4	9.8	20.1
	160#1	179.7	20.3	41.5
100 kV	20	22	3	5.7
	40	38.4	7.4	15
	80	80	19.7	35.3
	160#1	160	45.2	76.4

#1 The maximum thickness of soft tissue was assumed as that of a human body (chest examination).

#2 The digital values corresponding to these materials were determined so as to agree with those of soft tissue in the same row.

Fig. 10: Summary of fabricated equal-image-density materials. The left figure shows a photograph of the materials. The right table indicates the determined thickness of the materials.

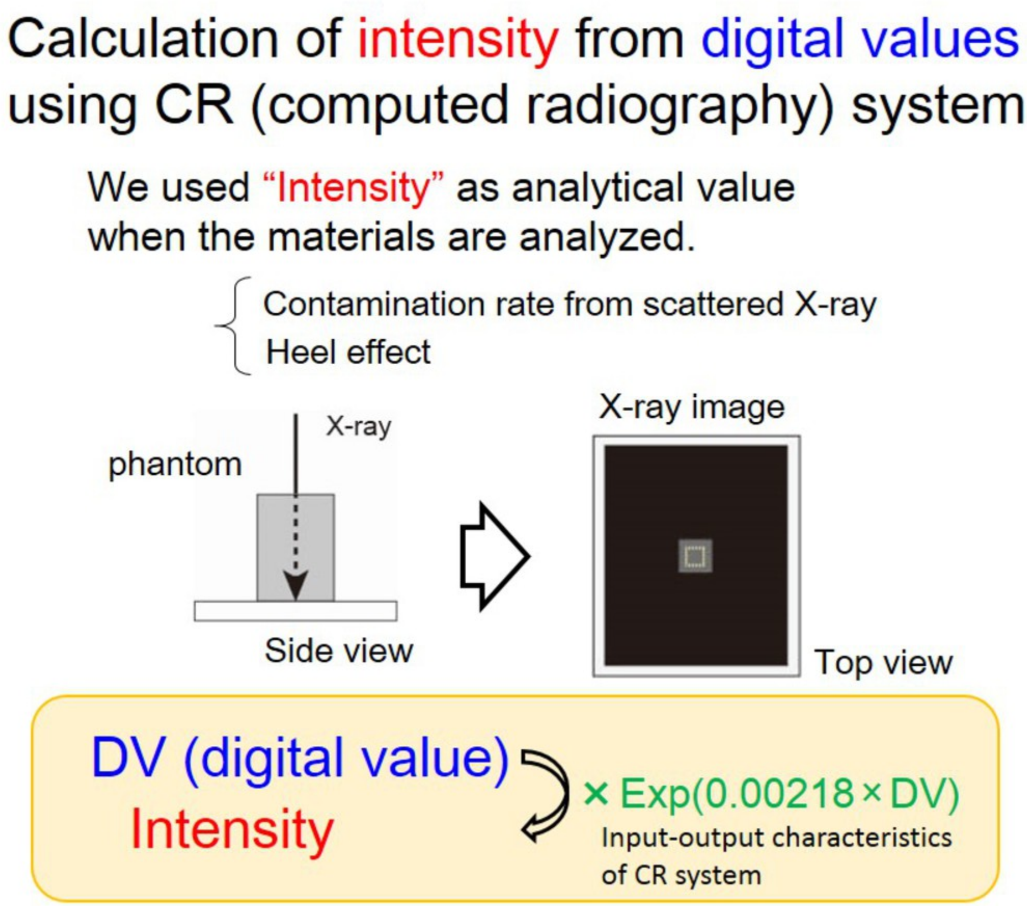

Fig. 11: Calculation methodology of intensity from digital value using CR system. Input-output characteristics of CR system were applied to convert intensity from the digital value.

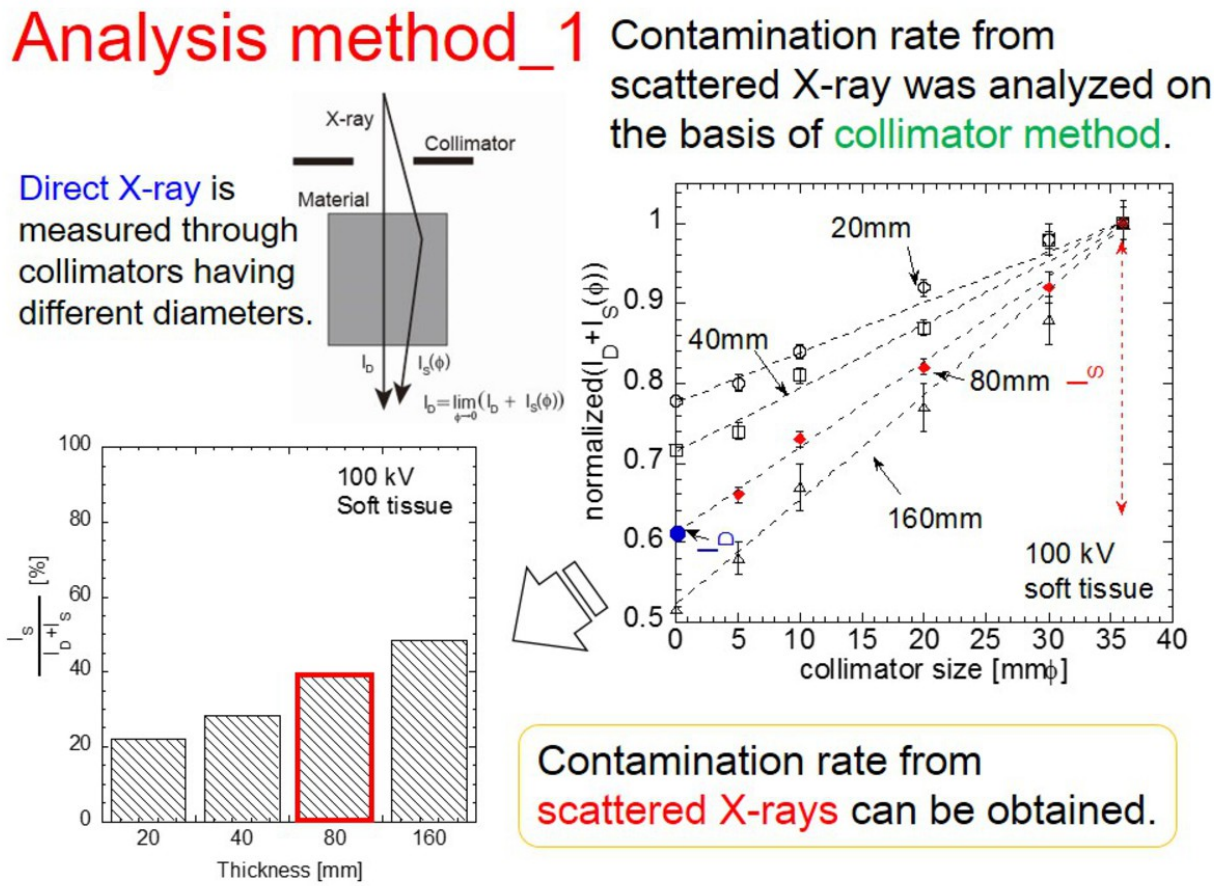

Fig. 12: Analysis methodology of contamination rate from scattered X-ray. Contamination rate from scattered X-ray is measured by collimator method.

© - Tokushima/JP

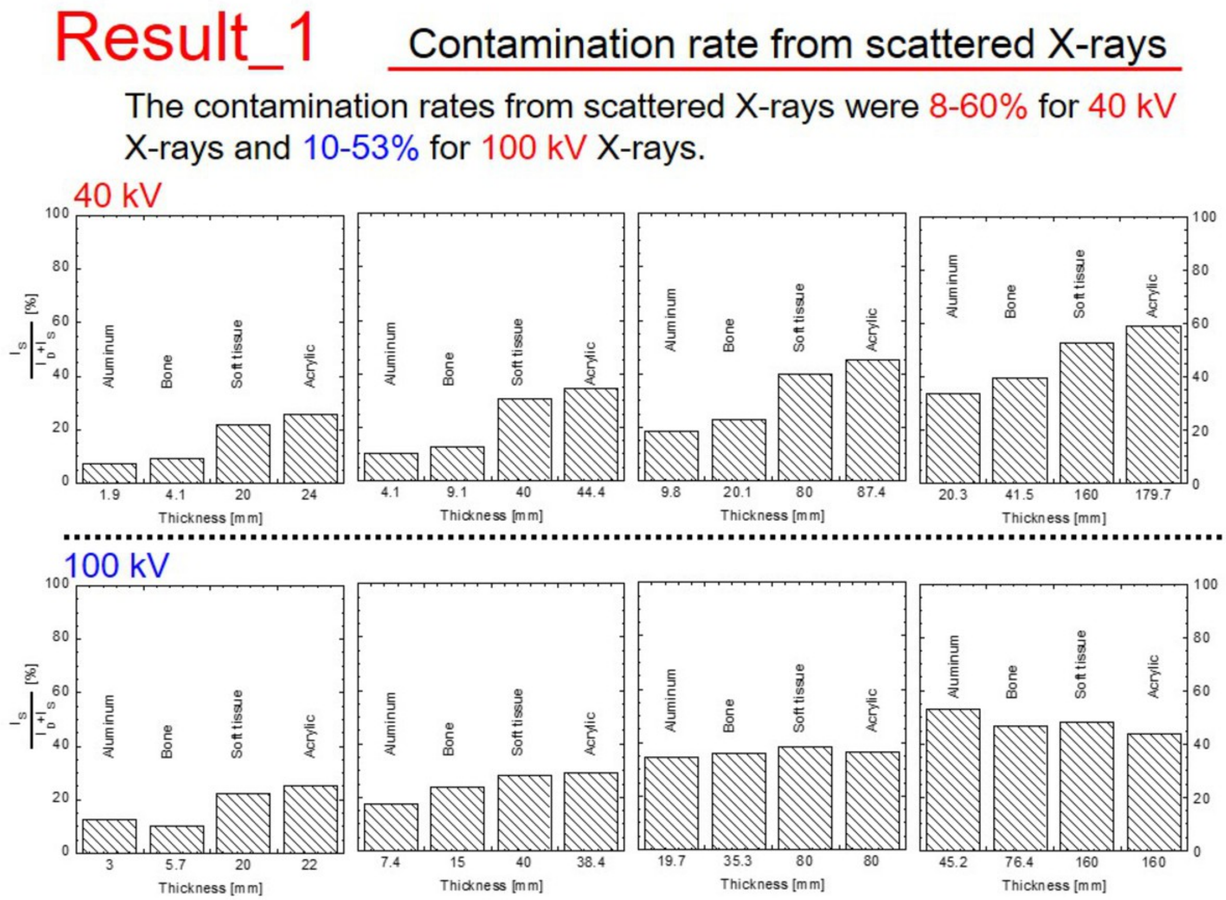

Fig. 13: Results of measured contamination rate from scattered X-ray.

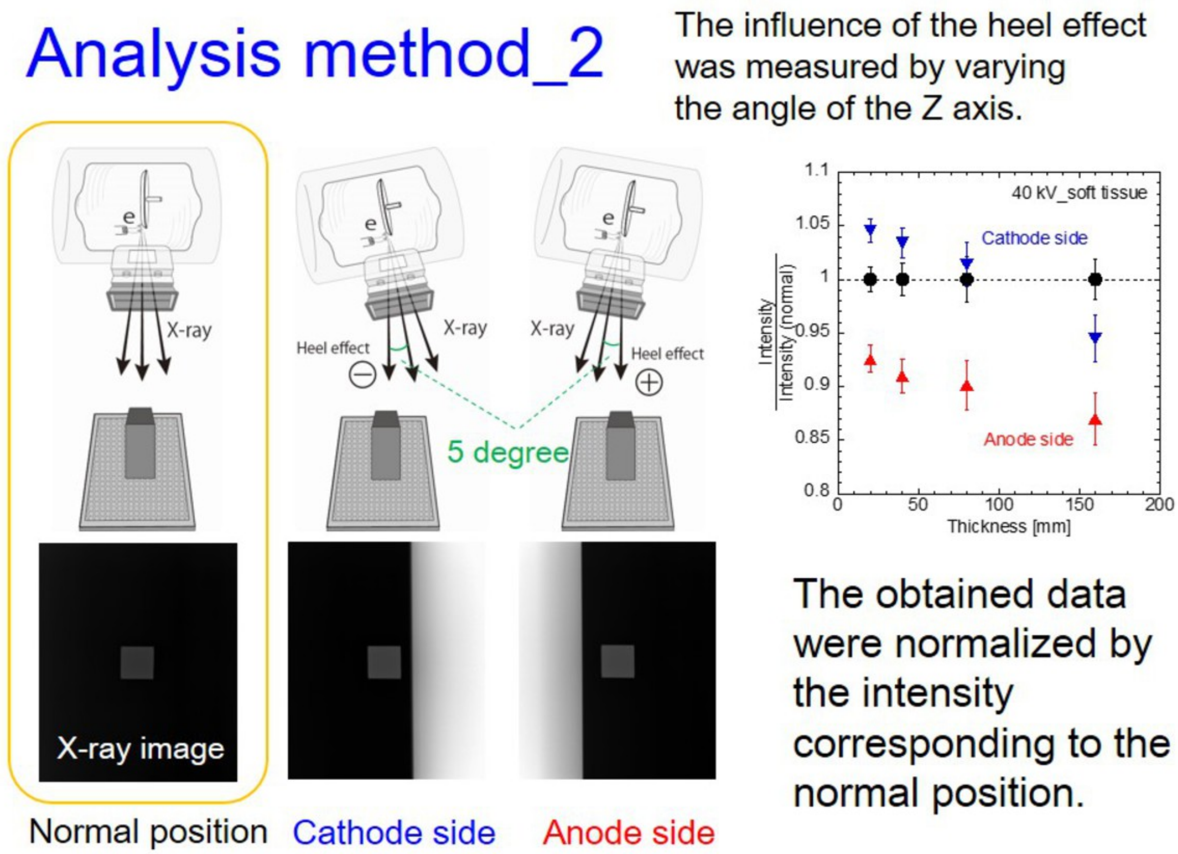

Fig. 14: Analysis methodology of heel effect on obtained image. The derived intensity is normalized by that of normal position.

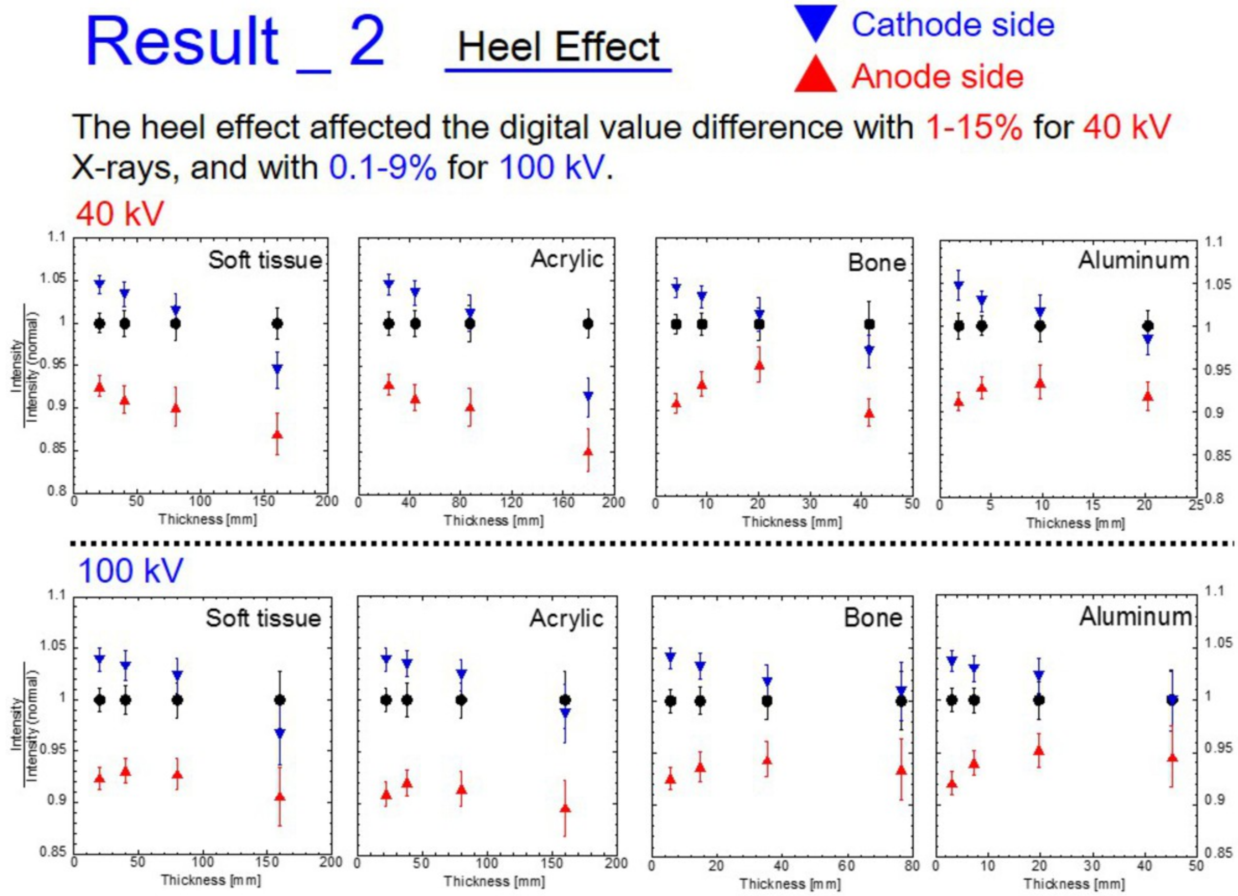

Fig. 15: Results of measured heel effect on obtained image.

Conclusion

Figure 16 summarized our study. In order to perform fundamental experiments for a photon counting technique, we fabricated equal-image-density materials for 40 kV and 100 kV X-rays using soft tissue, acrylic, aluminum and bone. The developed group of materials gave the same digital values when phosphor plate (CR system) was used as the X-ray detector. In the CR system, the digital value is determined by the amount of incident and scattered X-rays. Scattered X-rays vary as a function of phantom thickness, and incident X-rays are affected by the heel effect. Therefore, we examined their influence when using our fabricated materials. The experiments were carried out by means of clinically used diagnostic X-ray equipment. The contamination rate from scattered X-ray was determined by the collimator method. The heel effect on the obtained image was measured by an experiment in which the X-ray equipment was tilted at a 5 degree angle. As a result, we found that the contamination rate from scattered X-ray were 8-60 % for 40 kV X-rays and 10-53 % for 100 kV X-rays. For the heel effect the intensity differences were 1-15 % for 40 kV X-rays and 0.1-9 % for 100 kV X-rays. In **Figs. 17-24**, the thickness of fabricated materials and corresponding results of the experiments are presented. They are considered to be valuable for fundamental studies for next-generation detection systems such as a photon counting system.

Images for this section:

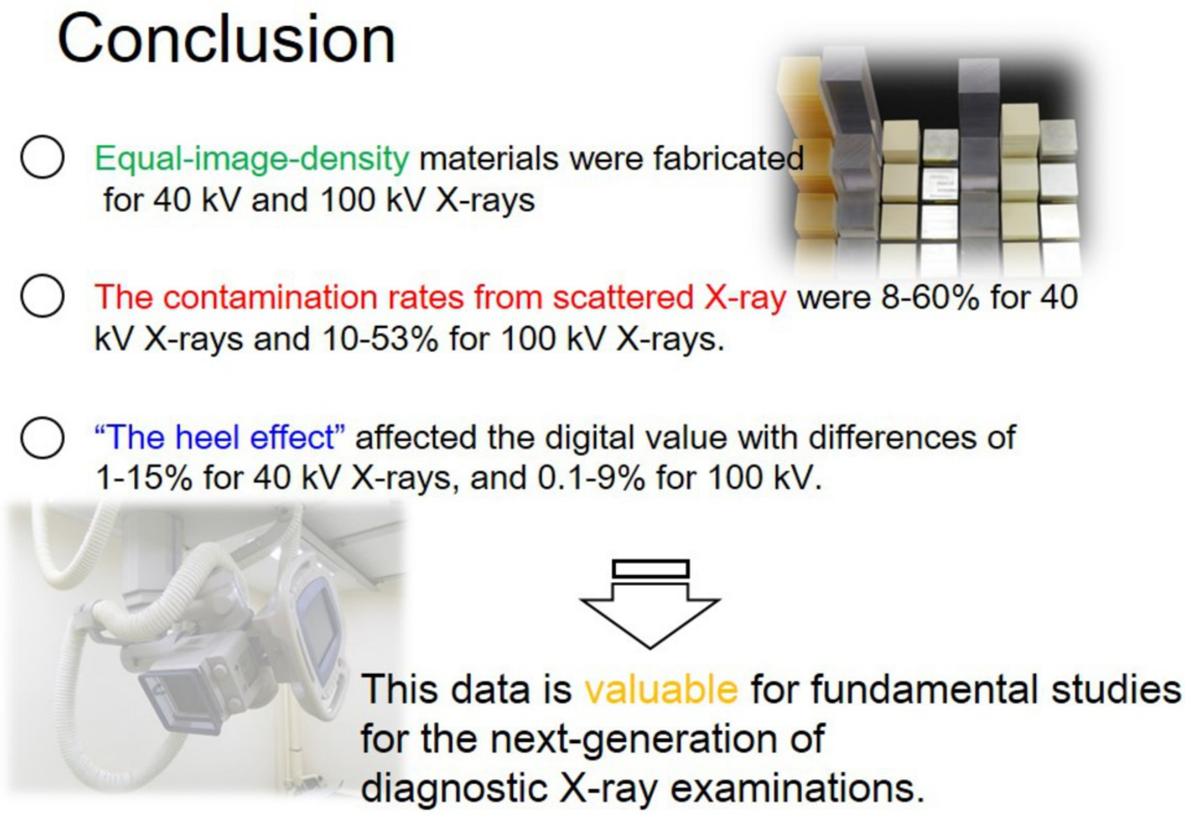

Fig. 16: Conclusion of our study.

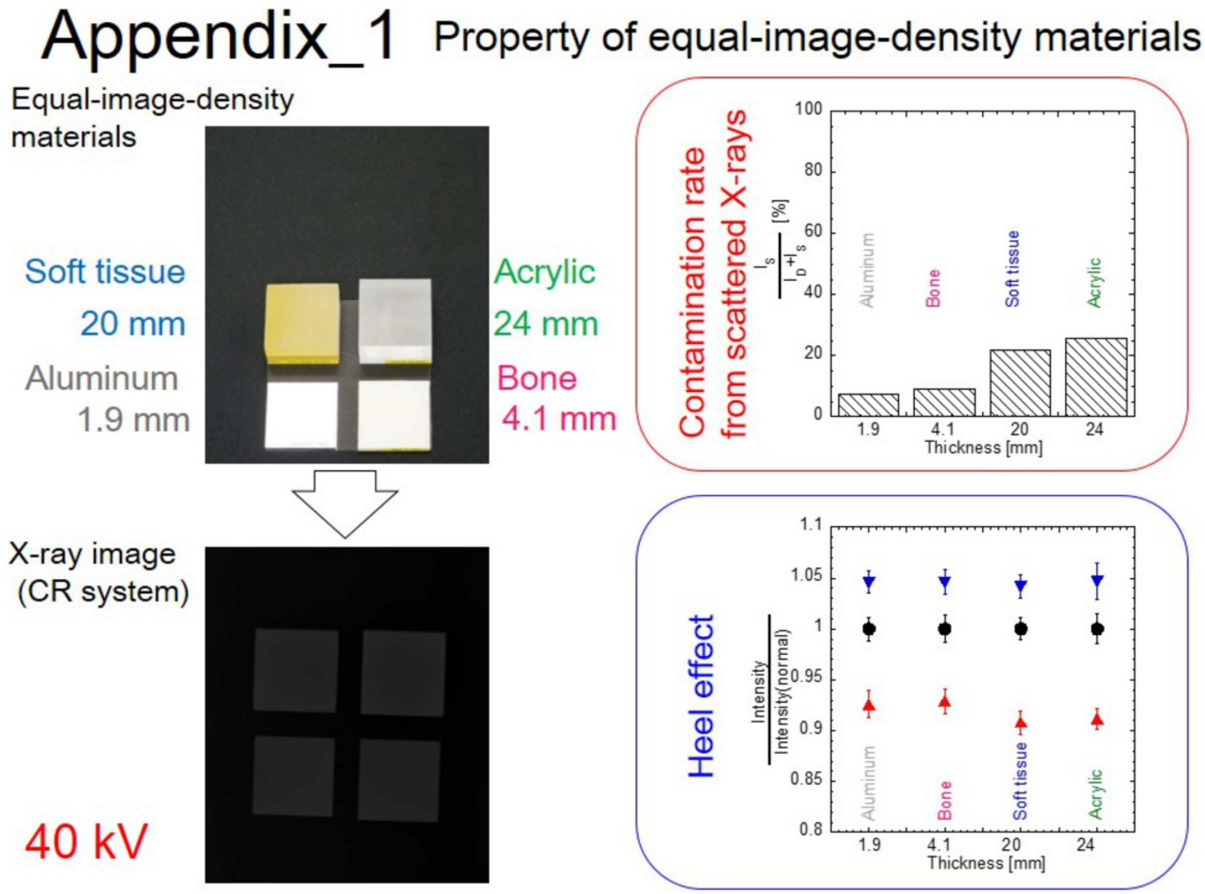

Fig. 17: Appendix of our study. Photographs and corresponding data of contamination rate from scattered X-ray and heel effect are presented.

© - Tokushima/JP

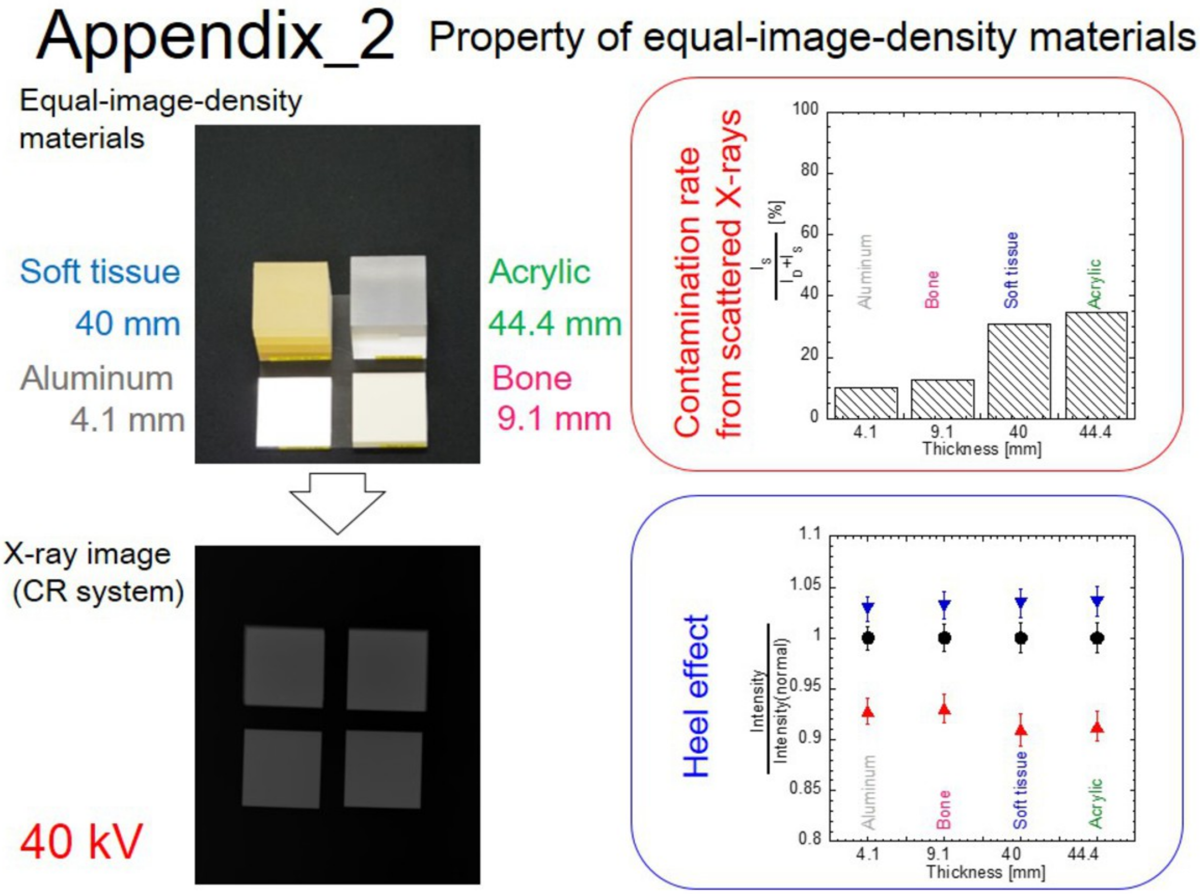

Fig. 18: Appendix of our study. Photographs and corresponding data of contamination rate from scattered X-ray and heel effect are presented.

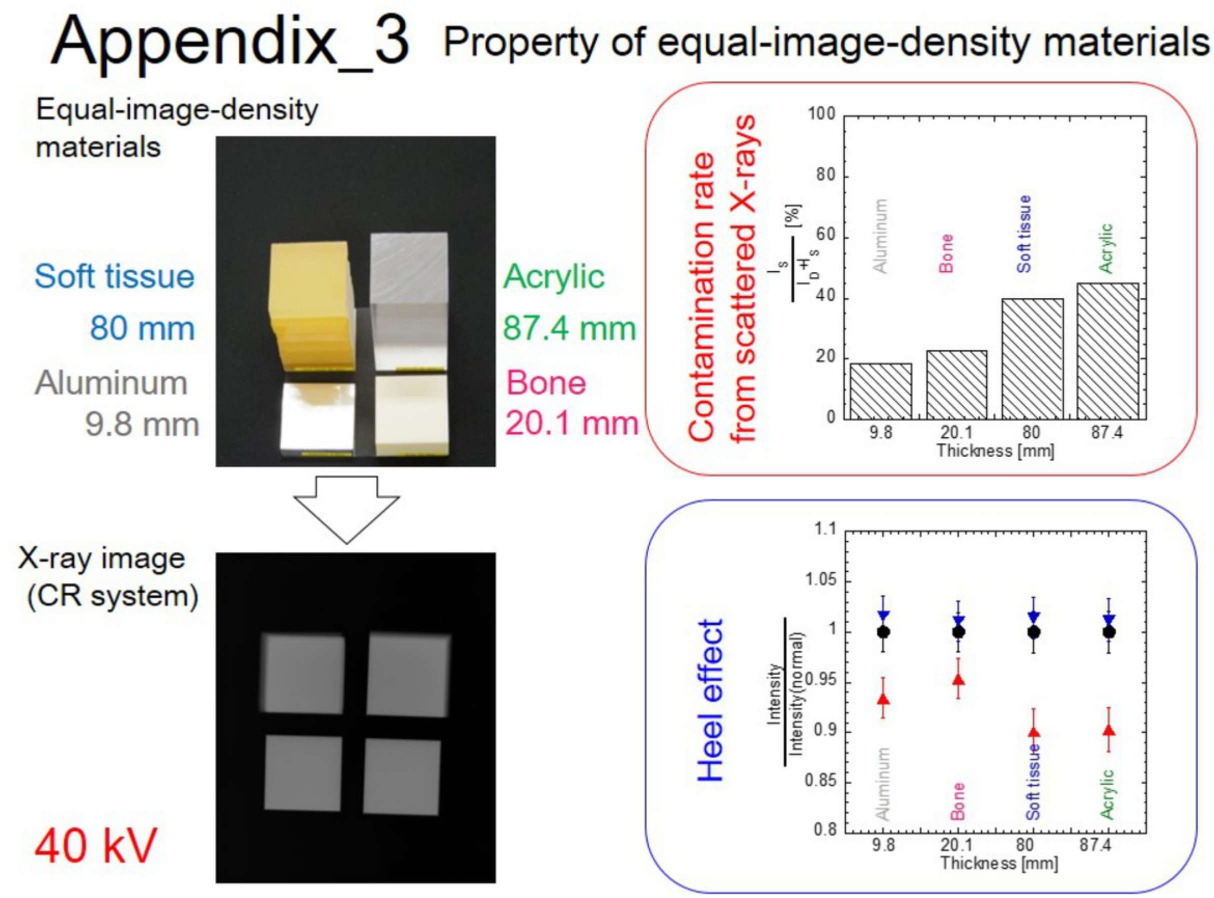

Fig. 19: Appendix of our study. Photographs and corresponding data of contamination rate from scattered X-ray and heel effect are presented.

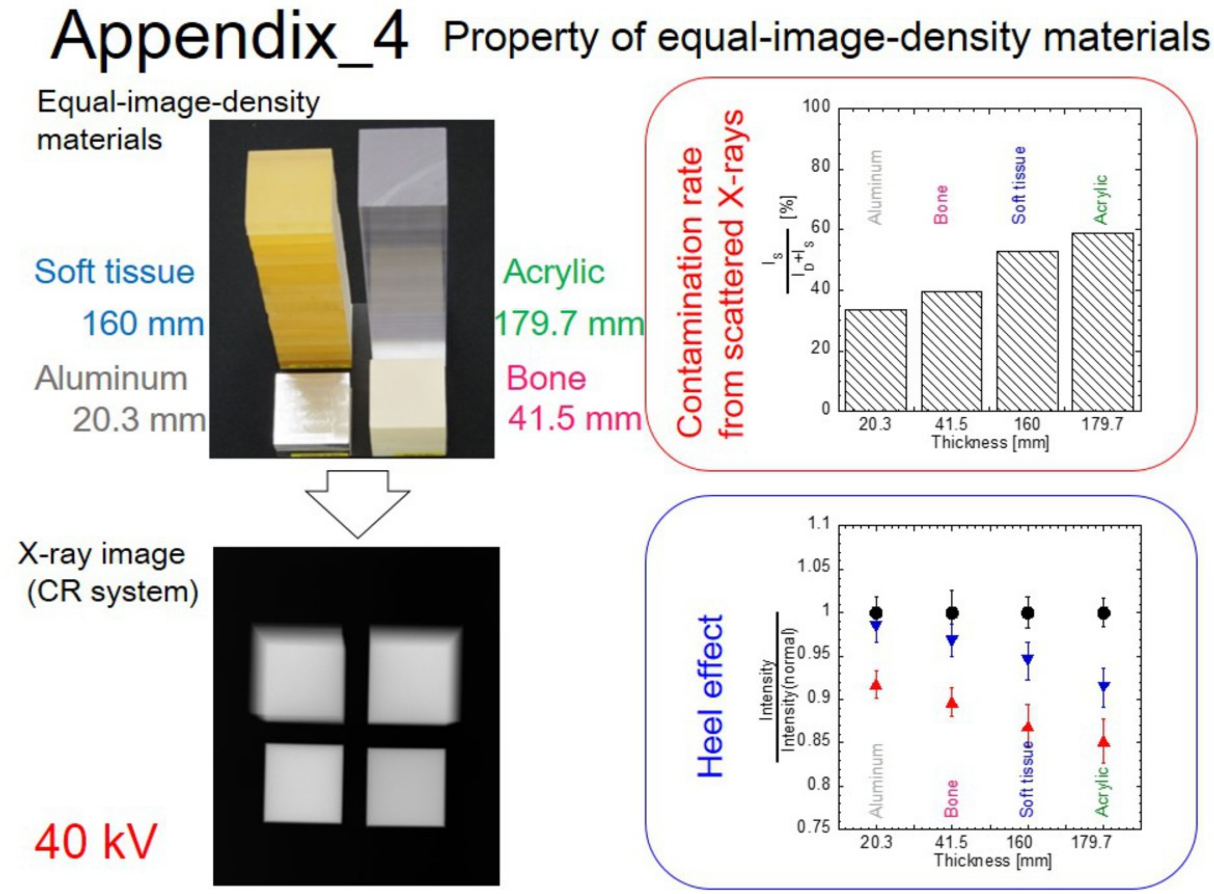

Fig. 20: Appendix of our study. Photographs and corresponding data of contamination rate from scattered X-ray and heel effect are presented.

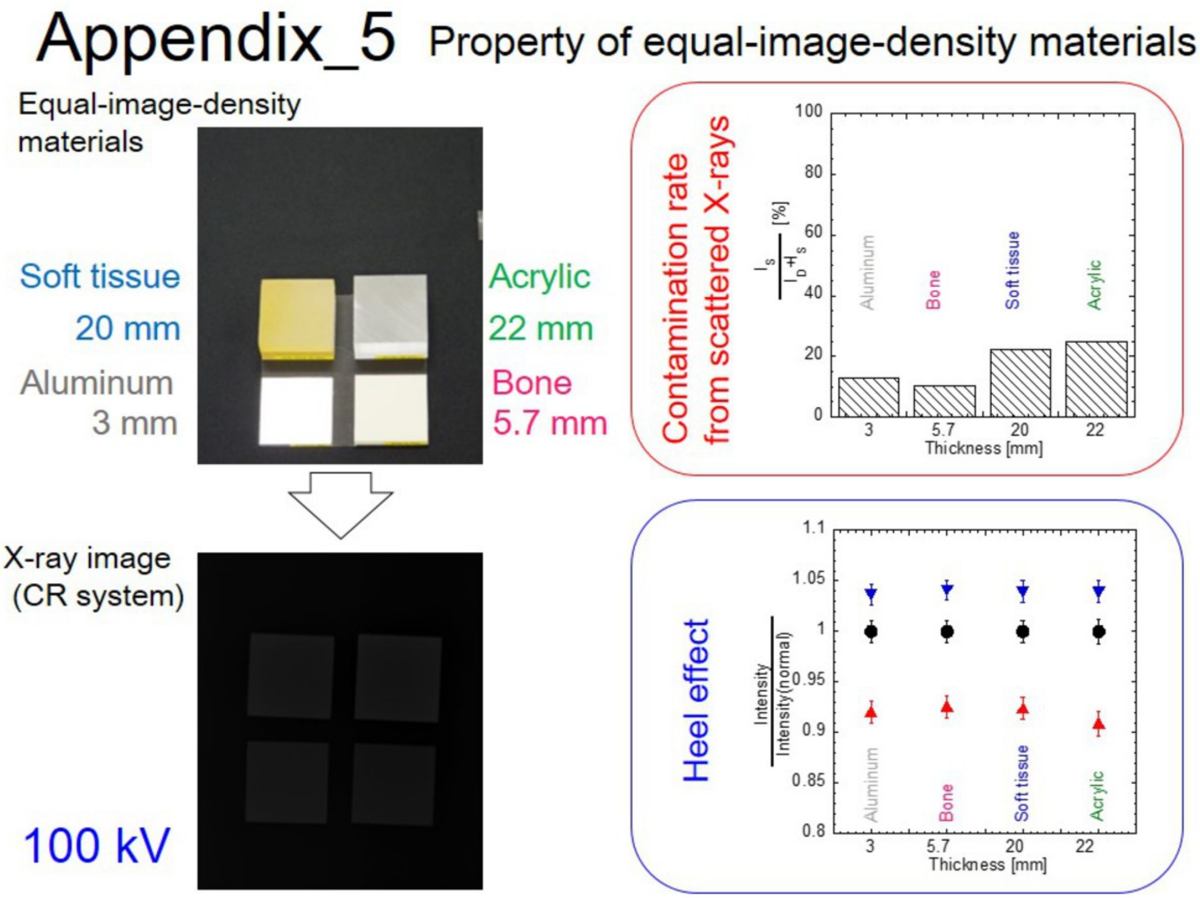

Fig. 21: Appendix of our study. Photographs and corresponding data of contamination rate from scattered X-ray and heel effect are presented.

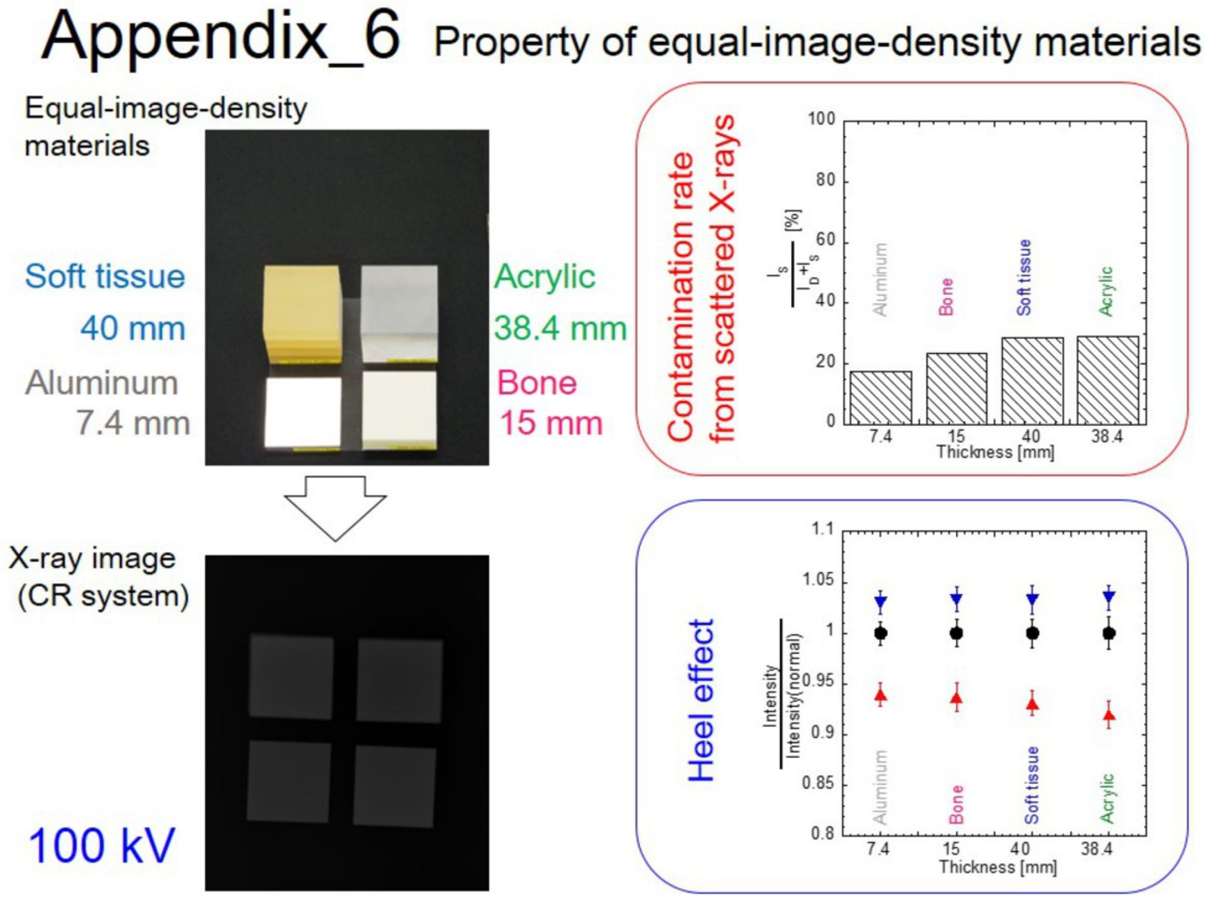

Fig. 22: Appendix of our study. Photographs and corresponding data of contamination rate from scattered X-ray and heel effect are presented.

© - Tokushima/JP

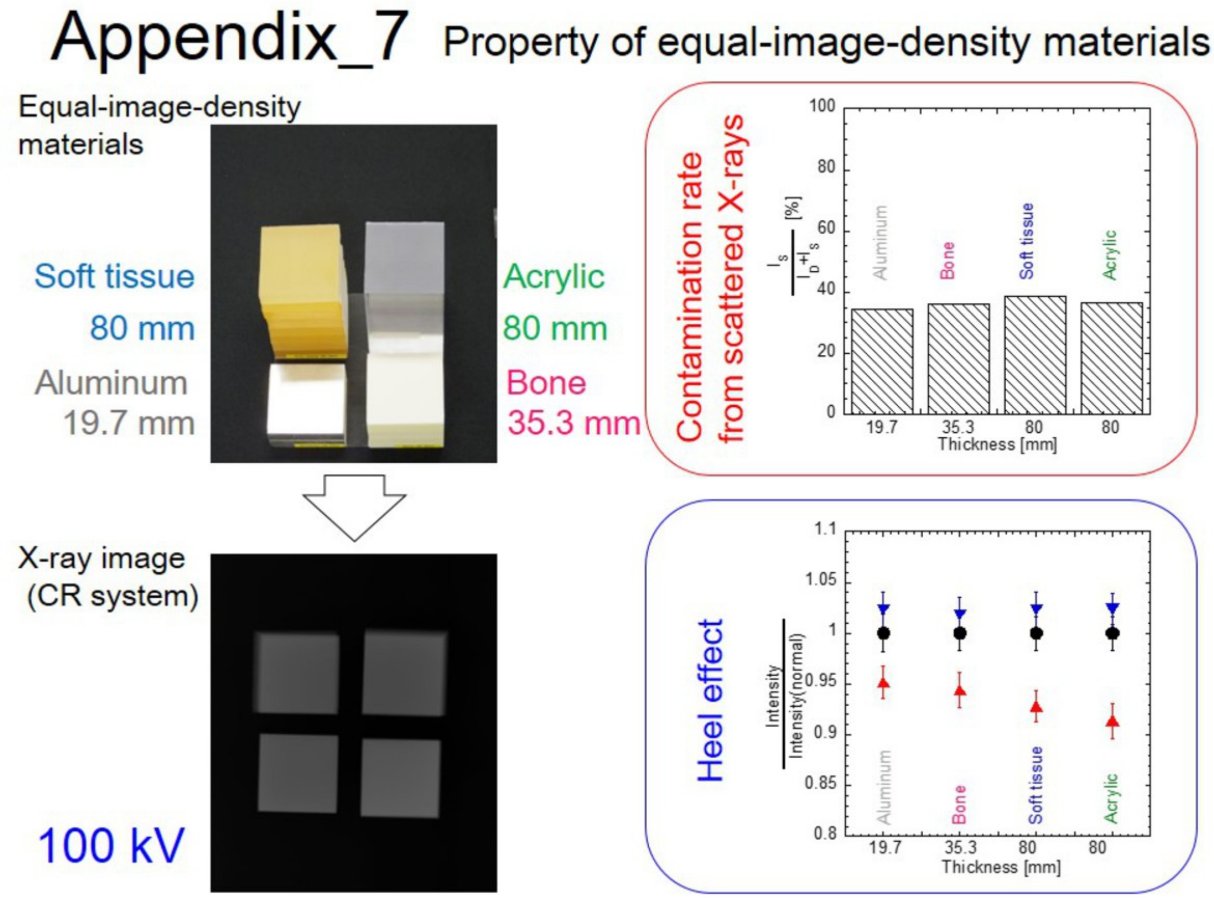

Fig. 23: Appendix of our study. Photographs and corresponding data of contamination rate from scattered X-ray and heel effect are presented.

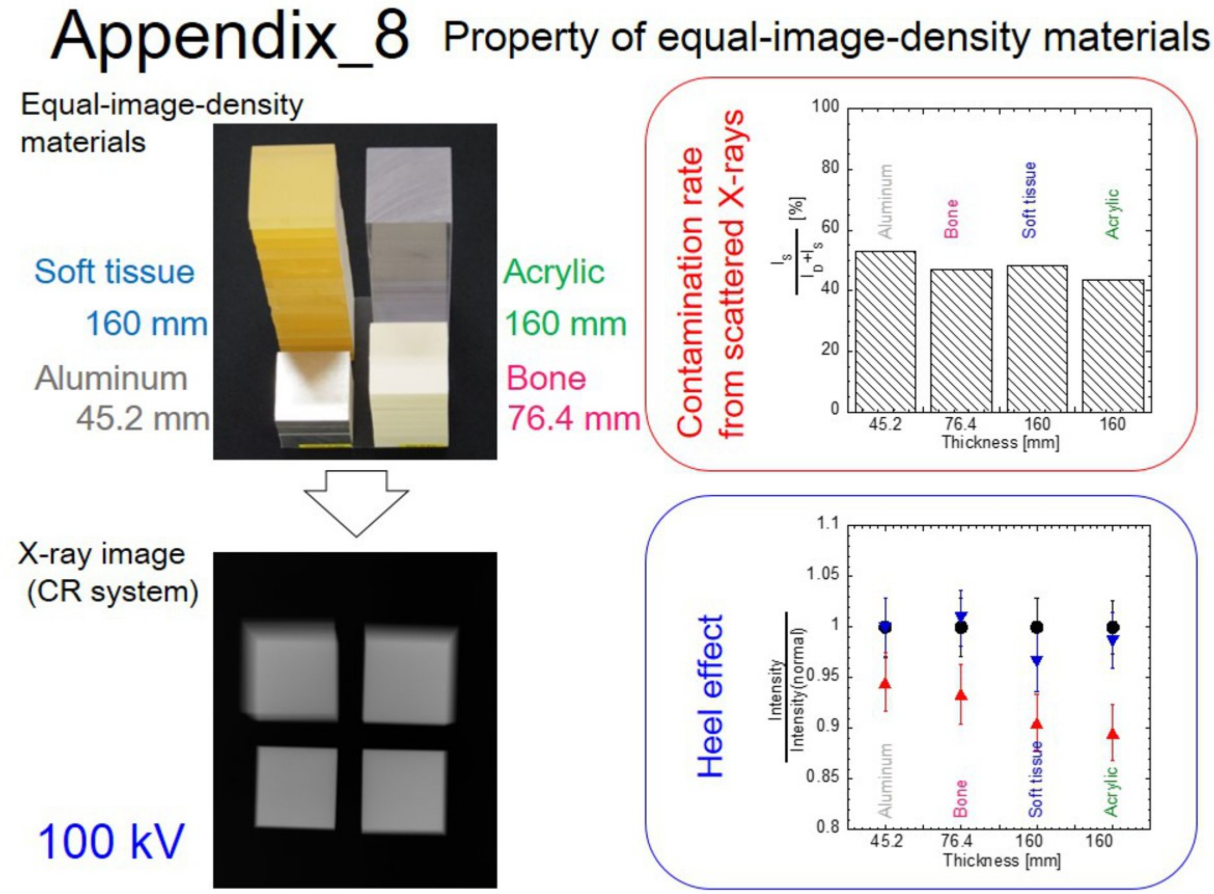

Fig. 24: Appendix of our study. Photographs and corresponding data of contamination rate from scattered X-ray and heel effect are presented.

Personal information

Name: Natsumi Kimoto

Affiliation: School of Health Sciences, Tokushima University, Japan

Email: c201204012@tokushima-u.ac.jp

References

[1] K. Taguchi, JS. Iwanczyk. Vision 20/20: Single photon counting x-ray detectors in medical imaging. Medical Physics 40, 100901, 2013.

[2] Seppi E., Zentai G., Partain L. *et al*., New method for breast tumor tracking, IEEE International Conference on Imaging Systems and Techniques, 442-445, 2012.

[3] Hasegawa B.H., Stebler B., Rutt B.K. *et al*., A prototype high-purity germanium detector system with fast photon-counting circuitry for medical imaging, Medical Physics, 18(5), 900-909, 1991.

[4] Schlomka J.P., Roessl E., Dorscheid R. *et al*., Experimental feasibility of multi-energy photon-counting K-edge imaging in pre-clinical computed tomography, Physics in Medicine and Biology, 53, 4031-4047, 2008.

[5] H. Hayashi, K. Takegami, Y. Konishi, *et al*., Indirect Method of Measuring the Scatter X-ray Fraction Using Collimators in the Diagnostic Domain, Japanese Journal of Radiological Technology, 70, 213-222, 2014.

[6] Fritz SL, Livingston WH. A comparison of computed and measured heel effect for various target angles. Medical Physics, 9, 216-219, 1982.

[7] Abramoff MD, Magelhaes PJ, Ram SJ. Image Processing with ImageJ. Biophotonics International, 11, 36-42, 2004.

[8] I. Maehata, H. Hayashi, K. Takegami, *et al*., Fabrication of Improved Multi-slit Equipment to Obtain the Input-output Characteristics of Computed Radiography

Systems: Correction of the Heel Effect and Application to High Tube-voltage Experiments, Japanese Journal of Radiological Technology, 70, 867-876, 2014.

[9] N. Kimoto, H. Hayashi, I. Maehata, *et al*., Development of All-in-one Multi-slit Equipment for Measurements of the Input-output Characteristic of a Phosphor Plate, Japanese Journal of Radiological Technology, 69, 1165-1171, 2013.